Pattern Recognition Letters
journal homepage: www.elsevier.com

A Tomographical Reconstruction Method from Unknown Direction Projections for 2D Gray-Level Images

Bassem Ben Cheikh[a], Étienne Baudrier[b,**], Gabriel Frey[b]

[a]*Sorbonne University, UPMC Univ Paris 06, UMR 7371, U1146, Lab. Imagerie Biomédicale, F-75013, Paris, France*
[b]*University of Strasbourg, CNRS ICube, 300 Bd Sébastien Brant, F-67412, Illkirch, France*

ABSTRACT

This paper deals with the reconstruction of gray level images from unoriented tomographic projections as it occurs in cryo-electron microscopy. Classical methods proceed in three steps: first, angular assignation, then image reconstruction from angular information and input projections and finally angular assignation refinement from the reconstructed image. We propose in this paper to perform the angular assignation and the image reconstruction at the same time. The main idea is to compare the input projections with the projections obtained from the image being reconstructed and the angular information. Our method is available for *ab initio* reconstruction and based on a cost optimization using the simulated annealing algorithm. A comparison with a state-of-the-art method (based on the spherical Local Linear Embedding) from the literature on a set of 2D gray-level images is done and it shows the better result of our method. The case where projections from different objects are acquired can also occur in cryo-electron microscopy (e.g. deformable molecule reconstruction). The feasibility of a reconstruction by our method in this case is shown on 2D images. Moreover our method can be generalized to the 3D case.

1. Introduction and State of the Art

The problem of tomographic reconstruction from projections with unknown directions is encountered in various domains such as medical imaging (e.g. when the patient is moving during an X-ray scanner acquisition) or cryo-Electron Microscopy (cryo-EM). In this latter mode of acquisition, a thin vitreous ice layer containing specimens of a macromolecule is magnified with an electron microscope. The orientations, relative to the microscope, of the specimens in the solution are not known. Thus the inputs of the object-reconstruction problem are 2D projections of a 3D object (later called input projections) whose relative views orientations are unknown. The image to reconstruct is a 3D image. This paper addresses the problem of reconstruction in the cryo-EM case but the method is presented for the (simpler) case of 2D gray-level image reconstruction. It extends our article focused on single object reconstruction (Ben Cheikh et al. (2014)) and explores the reconstruction feasibility in the case where the macromolecule is deformable and different macromolecule states are present in the observations.

The reconstruction problem with unknown directions is usually addressed in two stages (Crowther (1971); De Rosier and Klug (1968)): first, the projection directions are estimated, then the reconstruction itself is computed using the estimated directions (Frank (2006)). In his paper, Panaretos (2009) shows that the object density can be estimated without direction assignment under assumptions on it. Nevertheless, the proposed method is noise sensitive and has not been tested on real data which are noisy. In 3D, the estimation step relies on algorithms derived from common lines correlation (Bracewell (1956); Crowther (1971); Van Heel (1987)). In 2D, the projection slice theorem (Bracewell (1956)) which is the base of common line methods is no more useful. The distance used in this case is generally the Euclidean distance. Consistency of the projections moments has also been proved to lead to direction assignment recovery in 2D under certain assumptions (Basu and Bresler (2000); Goncharov and Gelfand (1988); Salzman (1990)). To cope with the high dimensional data space, direction assignment algorithms use dimension reduction (Coifman

**Corresponding author: Tel.: +33-(0)3 68 85 44 94;
e-mail: baudrier@unistra.fr (Étienne Baudrier)

et al. (2008); Fang et al. (2011)) or optimization (Elmlund et al. (2008); Ogura and Sato (2006)). For the reconstruction step, the main families of reconstruction methods are the algebraic methods, iterative filtered back projection, and those using the Fourier transform (Frank (2006)).

In the case where no previous reconstruction is available (so-called *ab initio* case), the sequence of these two steps gives a first reconstructed image whose quality is not always sufficient, and then requires a refinement step (Elmlund et al. (2008); Frank (2006)). The reconstructed image is used to refine the projection directions and these directions can then be used to improve the data reconstruction. This iteration reflects the fact that if the estimated directions influence the reconstruction of the image, the estimation of the image also affects the estimation of directions. Indeed, the refined image produces projections that can be then compared to input projections (from the acquisition equipment). Then, this allows to classify again the input projections. But this does not allow the estimated image to play its full role in the estimation of directions, since it is built later. We propose a method that offers this possibility. It is based on a simultaneous estimation of projection directions and image. Moreover, the proposed method does not require clustering or other supervised step and then the obtained reconstruction are not biased by some user's supervision. The method is presented for 2D gray-level images to show its feasibility.

The cryo-EM supposes the specimens of the macromolecule to be identical, but it occurs that distinct macromolecule conformations are found in the same sample; e.g. if the distinct conformations cannot be chemically separated. Therefore the single particle images have to be classified before the reconstruction step. Supervised classification is used to cope with this case. In such a classification, a projection image is assigned to a conformation and to a projection direction based on the 3D reference in the orientation producing the highest cross-correlation coefficient. The ability to retrieve several structures from the same sample even in the absence of specific reference structures has become one of the celebrated feats of single-particle cryo-EM (Schwander et al. (2014)). Our method has a promising extension for the reconstruction of multi-conformational molecule.

The paper is structured as follows: in Section 2, a model of the acquisition is shown and the problem is specified; in Section 3, the proposed method is detailed and the associated cost function is studied; in Section 4, the choice and the implementation of the optimization is presented; in Section 5 an extension to multi-object reconstruction is presented and evaluated then results are given in Section 6. Conclusion and perspectives end this paper.

2. Model and Problem

An acquisition in cryo-electron microscopy generates several images of the object acquired simultaneously in several directions. We assume here that the shortcomings of the acquired data (defocusing, contrast transfer function, aberrations, centers of gravity not placed at the origin of the coordinate system, etc.) have been corrected during pre-processing step. We first present the tomographical acquisition model for one direction, then for several directions.

For one direction, a parallel electron-beam is emitted and its intensity is measured after it went through the study object. This measured intensity is function of the object density (electronic density in the case of electron microscopy).

Let $B_2 = \{x \in \mathbb{R}^2 | \, \|x\| \leq 1\}$ be the unit ball of $\mathbb{R}^2$. We call K the set of the bounded measurable functions f (for the usual measure of Lebesgues) from the unit ball B_2 in $\mathbb{R}^+$ such that f is derivable and $\|\nabla f\|_1 = \int_{B_2} |\nabla f| < \infty$

Remark 2.1. As f is bounded,

$$\|f\|_2 = \int_{B_2} |f|^2 < \infty$$

Definition 2.2 (Projection). Let f be a function of K. The projection of the object f in the direction θ is a measurable function given by

$$\pi(f, \theta) \colon s \in \mathbb{R} \mapsto \int_{-1}^{1} f(s \cdot e^{i\theta} + t \cdot e^{i(\theta + \frac{\pi}{2})}) dt$$

The projection $\pi(f, \theta)$ is a bounded measurable function with support in $[-1, 1]$ and s is the distance to the origin.

Finally, let introduce an operator for the simultaneous acquisition of several projections. Let $n \in \mathbb{N}^*$ and $\Theta = (\theta_1, \ldots, \theta_n) \in \mathbb{S}^n$ where $\mathbb{S}$ is the planar angle set, we define the acquisition operator Π:

$$\Pi : (f, \Theta) \in K \times \mathbb{S}^n \mapsto \Pi(f, \Theta) = \{\pi(f, \theta), \theta \in \Theta\}$$

The set of all the projections $\Pi(f, \Theta)$ is called *sinogram.*

Remark 2.3. For $\tilde{\theta}_i = \theta_i \mod 2\pi$ such that $0 \leq \tilde{\theta}_i < 2\pi$, the set Θ is classically sorted such that $\tilde{\theta}_1 \leq \ldots \leq \tilde{\theta}_n$.

With these notations, the classical reconstruction process can be reformulated as follows:

1. an estimation $\hat{\Theta} = \{\hat{\theta}_1, \ldots, \hat{\theta}_n\}$ from the acquired projections $\{\pi_1 = \pi(f, \theta_1), \ldots \pi_n = \pi(f, \theta_n)\}$ for their directions,
2. a reconstruction of an object $\hat{f}$ from the oriented projections $\{(\pi_1, \hat{\theta}_1), \ldots, (\pi_n, \hat{\theta}_n)\}$.

In this process, the final result is the reconstructed object, the direction estimation being only an intermediate step. To account for the observation of the mutual influence between the direction estimation and the object reconstruction, we propose to jointly reconstruct the orientations and the object, which corresponds to the problematic:
From the input data $\{\pi_1, \ldots, \pi_n\}$**, find** $(\hat{f}, \hat{\Theta})$ **such that**

$$\Pi(\hat{f}, \hat{\Theta}) = \{\pi_1, \ldots, \pi_n\}. \tag{1}$$

The reconstructed object is obtained by selecting the first component $\hat{f}$ of the solution. As for the classical problem, the solution is defined modulo a rotation.

3. Method

Our solution to (1) is to provide an object f and directions $\Theta = \{\theta_1, \dots, \theta_n\}$ and evaluate them through a cost function $\boldsymbol{J_P}$ depending on the input projections $\boldsymbol{P} = \{\pi_1, \dots \pi_n\}$, taking as arguments an object and a set of directions (f, Θ) with positive values:

$$\boldsymbol{J_P} : \begin{cases} K \times \mathbb{S}^n & \to \mathbb{R}^+ \\ (f, \Theta) & \mapsto \boldsymbol{J_P}(f, \Theta) \end{cases}$$

Therefore, the solutions are estimated by computing:

$$(\hat{f}, \hat{\Theta}) = \text{argmin}_{f,\Theta} \boldsymbol{J_P}(f, \Theta) \tag{2}$$

The cost function $\boldsymbol{J_P}$ is based on three elements which are an image I, a set of directions Θ and the given projections. It is classically formed of a residual norm that estimates an error between the given projections $\boldsymbol{P}$ and projections $\{\pi(f, \theta), \theta \in \Theta\}$:

$$\boldsymbol{J_P}(f, \Theta) = \sum_{i=1}^{n} \|\pi_i - \pi(f, \theta_i)\|_2^2 \tag{3}$$

Remark 3.1. As the noise present in the electron microscopy data is Gaussian, the chosen $\mathbb{L}^2$ norm gives a robust estimator.

A discrete version of the cost function is presented below. We introduce the discrete gray-level image

$$f^r : \begin{cases} \mathbb{Z}^2 \to \mathbb{R}^+ \\ (i, j) \mapsto f^r(i, j) \end{cases}$$

such that

$$f^r(i, j) = \lfloor f(ri - 1/2, rj - 1/2) \rfloor$$

for all $(i, j) \in \mathbb{Z}^2$ where r is a positive real standing for the resolution and $\lfloor \cdot \rfloor$ is the integer part. As the continuous function f belongs to the function set K, its support is in the unit ball B_2, then

$$f^r(i, j) = 0 \text{ for } |i|, |j| \geq m \in \mathbb{Z}$$

where $m > M = \frac{1}{2r}$. We note

$$K^r = \{f^r | f \in K\} \ .$$

For $1 \leqslant i \leqslant n$, we denote $(P^r_{i,j})_{j=-M\dots M}$ a digitization of the given projection π_i and Π^r a digitization of the projection operator. Then

$$(Q^r_{i,j})_{j=-M\dots M} = \Pi^r(f^r, \theta_i)$$

is a digital projection. The matrices P^r and Q^r are digital sinograms. Note that Q^r depends on f^r and Θ. For a given resolution r, we define a digitization $\boldsymbol{J^r_P}$ of $\boldsymbol{J_P}$ as:

$$\boldsymbol{J^r_P}(P^r, f^r, \Theta) = \frac{1}{k^2 2Mn} \sum_{i=1}^{n} \sum_{j=-M}^{M} (P_{i,j} - Q_{i,j})^2, \tag{4}$$

where k is the number of gray levels.

This cost function has the following property of partial convexity.

Proposition 3.2 (Convexity on the pixel values). Let P^r be the set of projections of a function $f \in K$ against $\Theta = (\theta_1, \dots, \theta_n) \in \mathbb{S}^n$. Let a pixel $p \in \{1, \dots, n\}^2$ and a discrete function g^r_0. We define the operator $G^r_p : t \in \mathbb{R}^+ \mapsto G^r_p(t) \in K^r$ by

$$G^r_p(t) : q \in \{1, \dots, n\}^2 \mapsto g^r_0(q) + (t - g^r_0(p))\chi_{\{p\}}(q) \in \mathbb{R}^+$$

where χ_E is the characteristic function of the set E. Then the function

$$\varphi : t \in \mathbb{R}^+ \mapsto \boldsymbol{J^r_P}(P^r, G^r_p(t)), \Theta)$$

is convex.

In Proposition 3.2, g^r_0 stands for the current image and $G^r_p(t)$ is the current image whose value on the pixel p has been changed to t: for a pixel $q \neq p$, one has

$$G^r_p(t)(q) = g^r_0(q) + 0$$

and for the pixel p,

$$G^r_p(t)(p) = g^r_0(p) + (t - g^r_0(p)) = t \ .$$

Then the property reflects the convexity of the cost in function of the value at the pixel p. Its proof relies on the fact that the cost is a quadratic sum in function of the pixel values.

Proof. We prove the convexity of φ by showing that its second derivative is positive.

Let $u \in \mathbb{R}^+$, a direction index $i \in \{1, \dots, n\}$, a projection-pixel index $j \in \{-M, \dots, M\}$ and a pixel $p = (p_x, p_y)$.

Let first compute the derivative of

$$\alpha_{i,j} : t \mapsto P_{i,j} - Q_{i,j}(t),$$

where

$$Q_{i,j}(t) = \Pi^r(G^r_p(t), \theta_i) = \sum_{k=-M}^{M} \sum_{l=-M}^{M} \omega^{i,j}_{k,l} G^r_p(t)(k, l)$$

is the digital projection of $G^r_p(t))$ with $(\omega^{i,j}_{k,l})$ positive weights given by the projection operator. Then

$$\begin{aligned} \frac{\partial \alpha_{i,j}}{\partial t}(u) &= \frac{\partial (P_{i,j} - Q_{i,j})}{\partial t}|_u \\ &= -\frac{\partial Q_{i,j}}{\partial t}|_u \\ &= -\frac{\partial}{\partial t}\left(\sum_{k=-M}^{M} \sum_{l=-M}^{M} \omega^{i,j}_{k,l} G^r_p(k, l) \right)|_u \\ &= -\frac{\partial \omega^{i,j}_{p_x,p_y} G^r_p(p_x, p_y)}{\partial t}|_u \end{aligned}$$

then

$$\frac{\partial \alpha_{i,j}}{\partial t}(u) = -\omega^{i,j}_{p_x,p_y}, \tag{5}$$

and

$$\frac{\partial^2 \alpha_{i,j}}{\partial t^2}(u) = 0. \tag{6}$$

So, we have for φ

$$\frac{\partial^2 \boldsymbol{J}_{\boldsymbol{P}}^r(P^r, G_p^r, \Theta)}{\partial t^2}|_u = \frac{\partial^2}{\partial t^2}\left(\sum_{i=1}^{n}\sum_{j=-M}^{M} \|P_{i,j} - Q_{i,j}\|_2^2\right)|_u$$

$$= 2\sum_{1}^{n}\left(\left\|\frac{\partial(P_{i,j} - Q_{i,j})}{\partial t}|_u\right\|_2^2 + < P_{i,j} - Q_{i,j}, \frac{\partial^2(P_{i,j} - Q_{i,j})}{\partial t^2}|_u >\right)$$

where $<,>$ is the Euclidean scalar product. Then when replacing with $\alpha_{i,j}$, we obtain

$$\frac{\partial^2 \boldsymbol{J}_{\boldsymbol{P}}^r(P^r, G_p^r, \Theta)}{\partial t^2}|_u = 2\sum_{1}^{n}\left(\left\|\frac{\partial \alpha_{i,j}}{\partial t}|_u\right\|_2^2 + < \alpha_{i,j}, \frac{\partial^2 \alpha_{i,j}}{\partial t^2}|_u >\right)$$

with (5) and (6)

$$\frac{\partial^2 \boldsymbol{J}_{\boldsymbol{P}}^r(P^r, G_p^r, \Theta)}{\partial t^2}|_u = 2\sum_{1}^{n}(\omega_{p_x,p_y}^{i,j})^2.$$

Thus

$$\frac{\partial^2 \varphi}{\partial t^2}|_u = \frac{\partial^2 \boldsymbol{J}_{\boldsymbol{P}}^r(P^r, G_p^r, \Theta)}{\partial t^2}|_u > 0.$$

□

Proposition 3.2 helps to speed up the image convergence toward the minimum when the current directions are near the true directions.

4. Optimization

Even if the cost function $\boldsymbol{J}_{\boldsymbol{P}}^r$ is convex in function of the pixels values (Prop. 3.2), it is not convex in function of the direction values in general ; e.g. if an image f has two similar projections $\pi(f, \theta_i)$ and $\pi(f, \theta_j)$ (e.g. in the case of a symmetry) then permuting θ_i and θ_j in Θ will not change the cost value a lot and can correspond to a local minimum of the cost J_P^r. Deterministic optimization methods are not suitable for non-convex cost function since they likely give local minima. Thus we turn towards heuristic optimization methods. Several state-of-the-art methods have been tested and among these non-deterministic methods, the Simulated Annealing (SA) appears to give relevant results to minimize the cost $\boldsymbol{J}_{\boldsymbol{P}}^r$. It is an iterative optimization method based on the Metropolis algorithm (Kirkpatrick et al. (1983)). The algorithm starts from an initial state of the system with an initial temperature $T = T_0$. At each iteration of the SA, a modification of the system is proposed. This modification is evaluated by the cost function $\frac{\boldsymbol{J}_{\boldsymbol{P}}^r}{T}$ and causes a variation $\frac{\Delta \boldsymbol{J}_{\boldsymbol{P}}^r}{T}$. If the variation is negative, the proposed modification is accepted. Otherwise, it is accepted with a probability $e^{-\frac{\Delta \boldsymbol{J}_{\boldsymbol{P}}^r}{T}}$ (Metropolis rule). The temperature T decreases at each iteration toward zero following some annealing schedule. When the temperature T is high, the cost function $\frac{\boldsymbol{J}_{\boldsymbol{P}}^r}{T}$ is flat and allows almost all modifications to be accepted. Then variation amplitude of the cost function $\frac{\boldsymbol{J}_{\boldsymbol{P}}^r}{T}$ becomes bigger when the temperature T decreases, allowing less modifications.

At each iteration, the modification of the system (Im, Θ) is based on:

1. an elementary modification of the image Im by picking randomly a pixel and assigning to it a random gray-level value,
2. an elementary modification of the set Θ by selecting randomly a direction and assigning to it a random value (a number corresponding to a projection from the set $\boldsymbol{P}$).

The process stops when modifications are refused n_0 times. The algorithm of the minimization process is shown in Alg. 1 (for sake of simplicity, f^r is noted f). In order to gain efficiency, the search space is sampled.

Algorithm 1 Reconstruction algorithm

```
initialization f^(0), Θ^(0), T_0
while iter < sc_max do
    if iteration is pair then
        elementary modification of the current image f^crt
    else
        elementary modification of the current set Θ^crt
    end if
    if ΔJ_P < 0 then
        modification accepted
    else
        r ← random value ∈ [0, 1]
        if r < e^(−ΔJ_P / T) then
            modification accepted
        else
            modification rejected
            iter ← iter + 1
        end if
    end if
    T ← T_0 e^(−λT)
end while
return f^crt
```

Note that the indices of the projections $\{\pi_1, \ldots, \pi_n\}$ are arbitrary and as the direction set Θ is ordered only in function these indices, the values $\theta_1, \ldots, \theta_n$ are not ordered during the problem resolution.

Choice of Parameters

The parameters of the simulated annealing are:

- the initial temperature T_0,
- the cooling schedule,
- the initial state $(f^{(0)}, \Theta^{(0)})$,
- the stopping criterion sc_{max}.

Different types of temperature decay functions have been tested. The exponential decreasing functions give the better results with low decay rates λ and high initial temperatures T_0. The other parameters have been tuned for each resolution and each projection number so as to minimize the criterion of the average reconstruction error on a set of 50 images. The best parameters values depend on the image resolution and are gathered in Table 1.

Table 1. Optimal parameters of the simulated annealing in terms of image resolution. The number of the projections is twice the image size.

	16×16	32×32	64×64	128×128	256×256
decay rate λ	1	10^{-1}	10^{-3}	10^{-4}	10^{-5}
initial temperature T_0	1	10	10^2	10^3	10^3
convergence time	7 sec	22 sec	7.2 min	25.3 min	3h20min

These parameters values allow the algorithm to widely explore the research space and to converge robustly toward the solution of (2). It should be noted that the parameters used for the simulation come from a compromise between the quality of the reconstruction and the process duration. Several initial images have been tested but they don't affect the final reconstruction quality since the initial temperature chosen is high. Indeed, a high temperature allows almost any modification of the system therefore the properties given to the initial image can be totally lost after few iterations. The set of the initial directions $\Theta^{(0)}$ is chosen as a uniformly randomized sample. The optimization algorithm converges to a solution of (2) when the cost function $\boldsymbol{J}_{\boldsymbol{P}}^{r}$ approaches zero. As the cost function has many local minima, the algorithm may be trapped in one of these local minima and then cannot reach the optimal solution. Therefore we define another stopping criterion taking into account the number of consecutive iterations where the system does not change. Once a maximum number is reached the process is stopped. This number is set empirically to $sc_{max} = 200$ iterations.

The search space is large i.e. $(\{1,\dots,k\})^n \times ([0,\pi)^m$ where k is the number of gray levels, n the number of pixels, m the number of projections. Then we propose to sample the angular research space $[0,\pi)$ to reduce the research space and to improve the optimization. Under the hypothesis that the directions of the projections are uniformly distributed on $[0,\pi)$, we propose a regular sampling with a step of $\frac{\pi}{m}$. With this sampling, our search space comes down to $(\{1,\dots,k\})^n \times (\{1,\dots,m\})^m$. A big sampling step gives a smaller research space but increases the reconstruction error. Then the choice of a sampling step results from a compromise between the reconstruction error and the research space size.

Even if it is clear that the image and the directions influence each other, it is possible that their mutual influence is minor. Figure 1 offers the possibility to show the importance of the mutual influence on a reconstruction of an image. Let us note $c_{im}(i)$ the correlation between the original and the reconstructed image at the iteration i of the minimization process and $c_{dir}(i)$ the correlation between the original and the reconstructed projection directions also at the iteration i. Figure 1 represents the set of points $(c_{dir}(i), c_{im}(i))$, $1 \le i \le 140000$, where $i = 1$ stands for the first iteration of the optimization process and $i = 140000$ for the last one.

Between these two bounds, the optimization process can be cut in three parts:

1. a search part (bottom left part of the graph, points in dark blue),
2. a joint reconstruction of the directions and image (points in blue to cyan),
3. a part where direction reconstruction –almost done– is refined while the image reconstruction still progresses based on that directions, (cyan to red points).

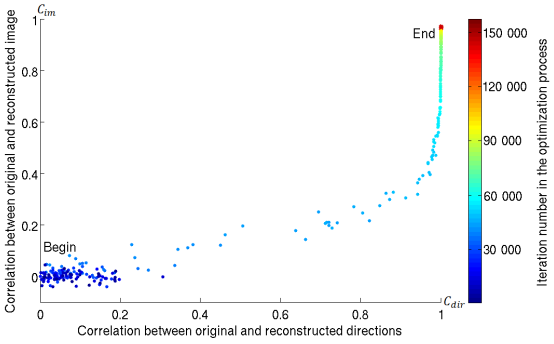

Fig. 1. On the abscissas (resp. on the ordinates), representation of the correlation between the original directions (resp. the original image) and the reconstructed projection directions (resp. the reconstructed image) for each step of the optimization process

The second part shows that the mutual influence is important in this reconstruction process. This mutual influence is not taken into account in the classical process which searches first the consistency between the projections (when estimating the directions).

5. Multiconformation Reconstruction

A macromolecular complex can present distinct conformations (or states). These conformations are of biological interest because they are often linked to the functions of the macromolecule. Therefore we present here an extension of our method to the case of multiconformation reconstruction. In this case, the projections are not only obtained from unknown angles but also from unknown conformations. In fact, each projection corresponds to one of the unknown states of the macromolecule.

The number of the conformations existing among the specimens is unknown and the number of projections per conformation is also unknown. But for the simplest, we supposed here that we initially have a set $\mathcal{P}$ of P data projections and we seek to reconstruct K images corresponding to K different states $f_1,\dots,f_K$ of the macromolecule. We also suppose that there exists a set of N projections per state, where $N \times K = P$. Thus, the problematic is:

From the input data set $\mathcal{P} = \{\pi_1,\dots,\pi_P\}$, for each $1 \le i \le K$ find $(\hat{f}_i, \hat{\Theta}_i)$ and a set $\{\pi_{i,1},\dots,\pi_{i,N}\} \subset \mathcal{P}$ such as

$$\Pi(\hat{f}_i, \hat{\Theta}_i) = \{\pi_{i,1},\dots,\pi_{i,N}\},$$

We propose to extend our method by reconstructing, from a large set of input data projections, not only a pair of object and directions $(\hat{f}, \hat{\Theta})$ but a set of pairs $\{(\hat{f}_1, \hat{\Theta}_1),\dots,(\hat{f}_K, \hat{\Theta}_K)\}$ jointly. To handle this, a set of objects $\{f_1,\dots,f_K\}$ and a set of current directions $\{\Theta_1,\dots,\Theta_K\}$ are provided, where $\Theta_i = \{\theta_{i,1},\dots,\theta_{i,N}\}$. The corresponding cost function $\boldsymbol{J}_{\mathcal{P}}$ is a sum wherein each term corresponds to the cost function $\boldsymbol{J}_{\boldsymbol{P}}$ defined in (3) to each image reconstruction:

$$\boldsymbol{J}_{\mathcal{P}}(\{f_1,\ldots,f_K\},\{\Theta_1,\ldots,\Theta_K\}) = \sum_{i=1}^{K}\sum_{n=1}^{N}\left\|\pi_{i,n} - \pi(f_i,\theta_{i,n})\right\|_2^2 \tag{7}$$

There is no cost computed between projections from distinct states, then the cost is computed as if the states were independent. At each iteration of the simulated annealing, the modification of the system $(\{f_1,\ldots,f_K\},\{\Theta_1,\ldots,\Theta_K\})$ is based on:

- (i) an elementary modification of the set of the images by selecting randomly an image and assigning a random gray-level value to a random pixel,
- (ii) an elementary modification of the set of the projections by selecting randomly a projection and assigning it to a random image and a random direction.

6. Results

6.1. Single Conformation Reconstruction Results

The proposed method has been applied to a set of 50 gray-level images of different resolutions (16×16, 32×32, 64×64, 128×128 and 256×256), referred to as phantoms. The phantoms are generated randomly by a Matlab program[1]. A set of projections uniformly distributed has been generated from the images. A random direction has been assigned to each projections.

There is not much methods in 2D to compare our results with because most of the methods are reconstruction methods with known angles. Fang et al. (2011) present a method that estimates the directions and reconstructs the object. The direction estimation is done by a spherical Local Linear Embedding (sLLE) method and the object reconstruction is done thanks to a filtered backprojection.

An illustration of image reconstructions by our method is presented in Figure 2 for a single image at different resolutions. We also reconstruct the images by Fang's method. It gives worser reconstruction results than our method. We provide a quantitative measure for the reconstruction performance which is the mean square error (MSE) between the phantom image and the reconstructed image. The MSE is normalized with the number of gray-scale and the area of the disk inscribed in the image support:

$$MSE = \frac{1}{k\pi(\frac{N}{2})^2}\sum_{i=1}^{N}\sum_{j=1}^{N}(I(i,j)-\hat{I}(i,j))^2 \tag{8}$$

Where I is the original image, $\hat{I}$ is the reconstructed image, N is the size of the images and k is the number of gray levels.

The reconstruction errors are presented in Figure 3. For each of the 50 phantoms, 10 reconstructions have been carried out and only the best one is retained. The best image corresponds to the reconstruction with the minimum cost value.

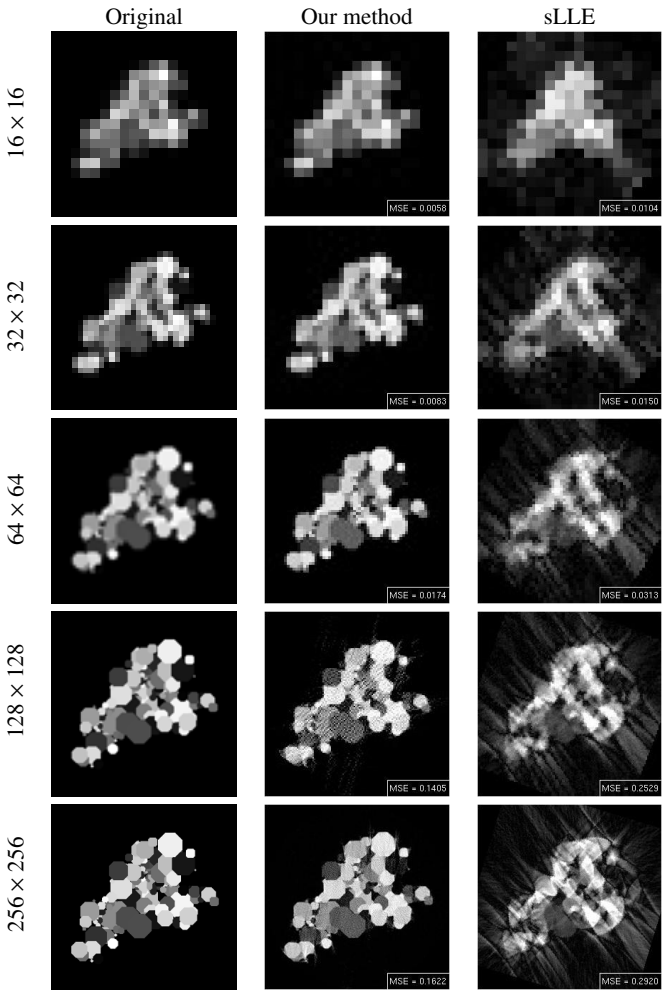

Fig. 2. A database image at different resolutions and its reconstructions by our method and by the method sLLE of Fang et al. (2011).

The robustness of the method against white noise has also been evaluated. A Gaussian noise with zero mean and standard deviation $\sigma = 5, 15$ and 50 has been added to the projections.

Example of reconstructions (Figure 4) and the reconstruction errors of phantoms of size 64×64 are shown for each noise level (Figure 5).The robustness of the method is good for low noise levels and the visual image quality decreases from the 40-standard deviation Gaussian noise. This behavior is logical as angular assignation is difficult from noisy projections. Moreover image reconstruction needs a larger number of projections with noise than without noise. This shows that our method need to pre-process the noisy projections to achieved a better robustness.

6.2. Multiconformation Reconstruction Results

The proposed method has been applied to 80 gray-level images of 128×128 pixels representing 20 macromolecules in several deformations[2]. A set of projections uniformly distributed

[1] Images and program are available at `http://rhodes;unistra.fr/en/images/c/cc/DB_50_gray_images_5_resol.zip/`

[2] Images are available at `http://www.molmovdb.org`

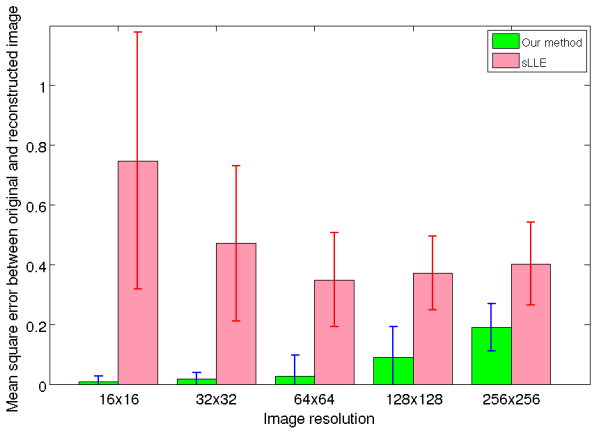

Fig. 3. Mean value and standard deviation (on 50 reconstructions) of the MSE between the reconstructed images and original images in function of the image size.

has been calculated from each image. As the image to which belongs a projection must be unknown, a random image index has been given to each projection and a random direction has been assigned to it.

For each of the 20 macromolecules, 20 reconstructions have been performed and only the best one (corresponding to the lower cost) was retained. Figure 6 shows reconstructed images by our method of four different states of the same macromolecule. The reconstructed image quality is still as good as in the single-conformation reconstruction case. The measure of reconstruction error used here is the same MSE as previously, applied to each state separately. The reconstruction errors are presented in Table 2.

Table 2. The Mean Square Error between the reconstructed images and the original images with different number of conformations and the corresponding Standard Deviations

Conformation number	1	2	3	4
Mean Square Error	0.089	0.261	0.374	0.416
Standard Deviation	0.069	0.094	0.093	0.091

The increase of the error with the number of conformations can be explained by the resemblance between some projections of different states which can generates an incorrect assignation of projections to an image and which can correspond to a local minimum of the cost function. These results show that the extension of our method to the *ab initio* reconstruction of several conformations is possible and it shows the path to the 3D multiconformation case.

7. Conclusion

This paper presents a new method for *ab initio* reconstruction of 2D gray level images. The proposed method assigns the projection orientations and reconstructs the image simultaneously. The process relies on the minimization of a residual norm between the original set of projections and the projections computed from the estimated image and directions. The

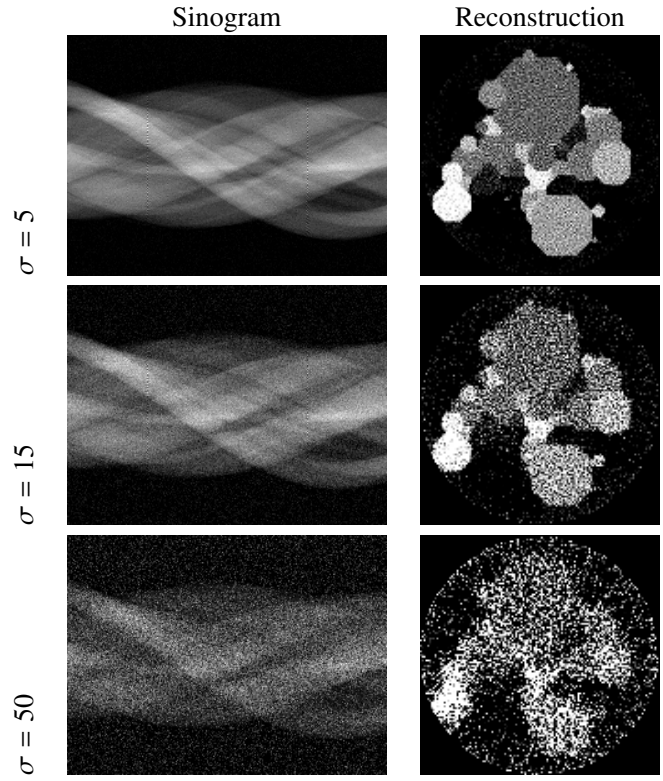

Fig. 4. For a single image, the sinogram is noised with Gaussian noise of variance $\sigma = 5, 15, 50$. The reconstruction by our method is shown for each noise level.

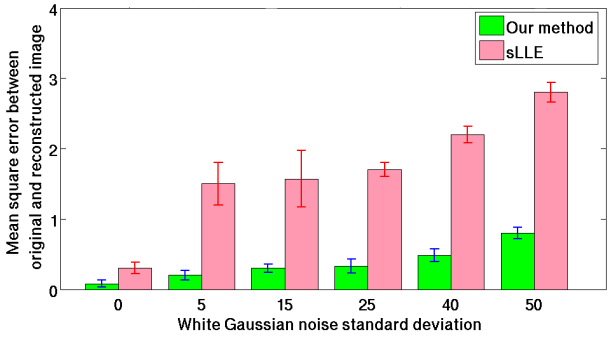

Fig. 5. Mean value and standard deviation of the wrong-pixels proportion in the reconstructed images in function of the additive Gaussian noise level.

optimization is made by a simulated annealing algorithm in a sampled direction space and does not require clustering or other supervised step.

Our method have been experimented on gray-level images at different resolutions and its robustness has been evaluated against different Gaussian noise levels. The results are good for an *ab initio* reconstruction method even without post-processing.

Instead of increasing the reconstruction number, we will take advantage of the good results of the low-resolutions by integrating them in a multi-resolution process in our future works.

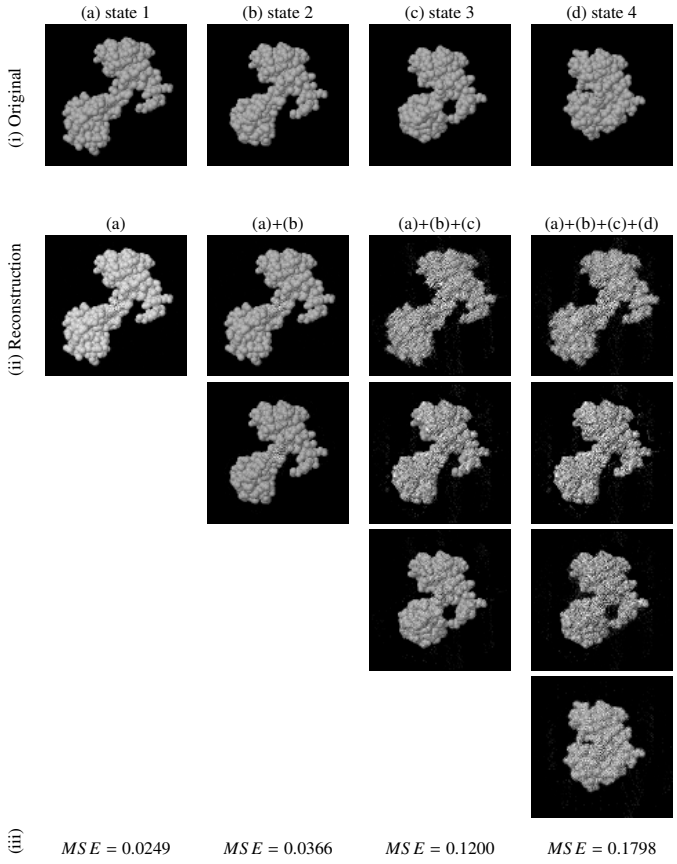

Fig. 6. (i) A macromolecular complex presented in different conformations. (ii) Its simultaneous reconstructions results. (iii) Global Mean Square Error of all reconstructions

Moreover, some experiments show the ability of our method to reconstruct deformable objects. The method will be extended to 3D objects in further works. Another perspective is to study and improve the cost function by introducing prior information on the set of projections (e.g. exploiting the Ludwig Helgason property Natterer (1986)) and on the image (e.g. smoothness).

References

Basu, S., Bresler, Y., 2000. Uniqueness of tomography with unknown view angles. IEEE T Image Process 9, 1094–1106.

Ben Cheikh, B., Baudrier, É., Frey, G., 2014. A tomographical reconstruction method from unknown direction projections for 2D gray-level images, in: 2014 IEEE 11th Int Symp on Biomed Imaging (ISBI), pp. 209–212.

Bracewell, R.N., 1956. Strip integration in radio astronomy. Aust J Phys 9, 198–217.

Coifman, R.R., Shkolnisky, Y., Sigworth, F.J., Singer, A., 2008. Graph laplacian tomography from unknown random projections. IEEE T Image Process 17, 1891–1899.

Crowther, R.A., 1971. Procedures for three-dimensional reconstruction of spherical viruses by Fourier synthesis from electron micrographs. Phils. Trans. R. Soc. Lond. B 261, 221–228.

De Rosier, D., Klug, A., 1968. Reconstruction of three dimensional structures from electron micrographs. Nature 217, 130–134.

Elmlund, H., Lundqvist, J., Al-Karadaghi, S., Hansson, M., Hebert, H., Lindahl, M., 2008. A new cryo-em single-particle ab initio reconstruction method visualizes secondary structure elements in an atp-fueled aaa+ motor. J Mol Biol 375, 934–947.

Fang, Y., Vishwanathan, S.V.N., Sun, M., Ramani, K., 2011. sLLE: Spherical Locally Linear Embedding with Applications to Tomography. CVPR , 1129–1136.

Frank, J., 2006. Three-Dimensional Electron Microscopy of Macromolecular Assemblies. Oxford University Press, New York.

Goncharov, A., Gelfand, M., 1988. Determination of mutual orientation of identical particles from their projections by the moments method. Ultramicroscopy 25, 317 – 327.

Kirkpatrick, S., Gelatt, C.D., Vecchi, M.P., 1983. Optimization by simulated annealing. Science 220, 671–680.

Natterer, F., 1986. The Mathematics of Computerized Tomography. John Wiley & Sons.

Ogura, T., Sato, C., 2006. A fully automatic 3D reconstruction method using simulated annealing enables accurate posterioric angular assignment of protein projections. J Struct Biol 156, 371 – 386.

Panaretos, V.M., 2009. On random tomography with unobservable projection angles. Ann Stat 37, 3272–3306.

Salzman, D., 1990. A method of general moments for orienting 2D projections of unknown 3D objects. Comput., Vis., Graph., Image Process. 50, 129–156.

Schwander, P., Fung, R., Ourmazd, A., 2014. Conformations of macromolecules and their complexes from heterogeneous datasets. Philosophical Transactions of the Royal Society B: Biological Sciences 369, 20130567.

Van Heel, M., 1987. Angular reconstitution: A posteriori assignment of projection directions for 3d reconstruction. Ultramicroscopy 21, 111–123.